Earthquakes and Structures, *Vol. 18, No. 2 (2020) 263-273*
DOI: https://doi.org/10.12989/eas.2020.18.2.263

Computing input energy response of MDOF systems to actual ground motions based on modal contributions

Taner Ucar*

Department of Architecture, Dokuz Eylul University, 35390, Buca, Izmir, Turkey

(*Received August 3, 2019, Revised December 27, 2019, Accepted January 18, 2020*)

Abstract. The use of energy concepts in seismic analysis and design of structures requires the understanding of the input energy response of multi-degree-of-freedom (MDOF) systems subjected to strong ground motions. For design purposes and non-time consuming analysis, however, it would be beneficial to associate the input energy response of MDOF systems with those of single-degree-of-freedom (SDOF) systems. In this paper, the theoretical formulation of energy input to MDOF systems is developed on the basis that only a particular portion of the total mass distributed among floor levels is effective in the *n*th-mode response. The input energy response histories of several reinforced concrete frames subjected to a set of eleven horizontal acceleration histories selected from actual recorded events and scaled in time domain are obtained. The contribution of the fundamental mode to the total input energy response of MDOF frames is demonstrated both graphically and numerically. The input energy of the fundamental mode is found to be a good indicator of the total energy input to two-dimensional regular MDOF structures. The numerical results computed by the proposed formulation are verified with relative input energy time histories directly computed from linear time history analysis. Finally, the elastic input energies are compared with those computed from time history analysis of nonlinear MDOF systems.

Keywords: input energy response history; time history analysis; MDOF system; *n*th-mode SDOF system; fundamental mode

1. Introduction

As a result of numerous efforts to achieve more effective and rational seismic design, energy-based procedures have become promising alternatives to conventional seismic design methods in recent years. In energy-based methods, structural seismic design is basically achieved through providing an adequate capacity to structural elements in comparison to seismic demand, which are both expressed in terms of energy (i.e., integral of force over displacement). Since the capacity of structural components is not exactly independent of loading history, the loading effect of earthquake also depends on structural characteristic. In this manner, the above mentioned shortcomings of force- and displacement-based design methods are overcome by interpreting the loading effect of earthquakes on structures as input energy, rather than considering forces and displacements separately.

Since the seismic energy imposed on a structure by earthquakes is balanced by providing adequate dissipation capacity, the first task to be considered in energy-based procedures is the precise calculation of input energy. Accordingly, several studies concerning seismic input energy to structures are available in scientific literature. These works mainly focus on development of design input energy spectra (Decanini and Mollaioli 1998, Benavent-Climent *et al*. 2002, Ordaz *et al*. 2003, Amiri *et al*. 2008, Benavent-Climent *et al*. 2010, Okur and Erberik 2012, López-Almansa *et al*. 2013, Cheng *et al*. 2014, Dindar *et al*. 2015, Alıcı and Sucuoğlu 2016, 2018, Quinde *et al*. 2016, Güllü *et al*. 2017, 2019, Zhou *et al*. 2019), as well as the use of absolute and relative energy in seismic design and assessment of structures (Wong and Yang 2002, Sari 2003, Surahman 2007, Kalkan and Kunnath 2008, Ye *et al*. 2009, Tselentis *et al*. 2010, Habibi *et al*. 2013, Shiwua and Rutman 2016, Mezgebo and Lui 2017, Yang *et al*. 2018, Merter 2019). Furthermore, energy demands imposed on structures by strong ground motions and the influence of various structural (e.g. hysteretic model, ductility ratio, damping ratio) and earthquake characteristics (e.g., intensity, frequency content, source-to-site distance, soil type, duration, fling step and forward directivity effects) were widely investigated (Manfredi 2001, Decanini and Mollaioli 2001, Hori and Inoue 2002, Chou and Uang 2003, Kalkan and Kunnath 2007, Taflampas *et al*. 2008, Mollaioli *et al*. 2011, Kanno *et al*. 2012, Mezgebo, and Lui 2016, Ozsarac *et al*. 2017, Gharehbaghi *et al*. 2018, Karimzadeh *et al*. 2019).

Unlike the extensive literature on seismic energy input to single-degree-of-freedom (SDOF) systems, studies concerning seismic energy demands in multi-degree-of-freedom (MDOF) systems are relatively limited. Estimation of earthquake input energy to MDOF systems and evaluating the distribution of input energy in MDOF systems were specifically studied (Decanini *et al*. 2001, Chou and Uang 2004, Takewaki 2004, Lei *et al*. 2008, Takewaki and Fujita 2009, Shargh and Hosseini 2011,

*Corresponding author, Associate Professor
E-mail: taner.ucar@deu.edu.tr

ISSN: 2092-7614 (Print), 2092-7622 (Online)

Takewaki and Tsujimoto 2011, Shargh *et al*. 2012, Mezgebo 2015, Beiraghi 2018, Ganjavi and Rezagholilou 2018, Morales-Beltran *et al*. 2018). It is noteworthy to mention that the input energy response of MDOF system is occasionally estimated from the input energy of the equivalent SDOF system (Decanini *et al*. 2001, Kalkan and Kunnath 2007, Mezgebo 2015, Mezgebo and Lui 2017).

It is quite imperative to practically estimate the earthquake energy input to MDOF systems, particularly for seismic design. Probably the simplest way to achieve this task is to associate the seismic energy response of MDOF systems with those of SDOF systems. Although not exactly corresponding to nonlinear input energy, reliable estimation of earthquake energy input is quite essential, since it has been shown that elastic input energy is well correlated to nonlinear response of structures and can also be used in estimating inelastic seismic demands (Mollaioli *et al*. 2011). Hence, an attempt to formulate the energy input to an MDOF system in terms of input energies of the *n*th-mode SDOF system is made. Input energy response histories of different MDOF systems are obtained by combining the modal analysis results of MDOF systems with velocity response history of *n*th-mode SDOF system and verified with those computed from linear time history analysis. The contribution of the individual modes, particularly of the fundamental mode, to input energy imposed by earthquake on MDOF structures is investigated. Finally, energy response histories of nonlinear systems are obtained.

2. Formulation of energy input to MDOF systems

The energy balance equation of a lumped mass linear elastic SDOF system subjected to horizontal earthquake excitation can be obtained by integrating the governing equation of motion of the system over the relative displacement of the mass:

$$\int_0^u m\cdot\ddot{u}(t)\,du+\int_0^u c\cdot\dot{u}(t)\,du+\int_0^u k\cdot u(t)\,du=-\int_0^u m\cdot\ddot{u}_g(t)\,du \quad (1)$$

where m is the mass of SDOF system, c is the viscous damping coefficient, k is the lateral stiffness of the system, u is the relative displacement of the system with respect to base and $\ddot{u}_g(t)$ is the ground acceleration.

For time domain numerical integration, Eq. (1) can be rearranged as in Eq. (2) by introducing $du=\dot{u}(t)dt$

$$\int_0^t m\cdot\ddot{u}(t)\cdot\dot{u}(t)\,dt+\int_0^t c\cdot\dot{u}^2(t)\,dt+\int_0^t k\cdot u(t)\cdot\dot{u}(t)\,dt=-\int_0^t m\cdot\ddot{u}_g(t)\cdot\dot{u}(t)\,dt \quad (2)$$

where t is the total duration of ground motion record. The energy response parameter on the right-hand side of Eq. (2) represents the relative earthquake input energy (E_I), which is the main concern of the study.

It is well known from the dynamics of SDOF systems that the relative displacement $u(t)$ of the mass subjected to horizontal ground acceleration is identical to the displacement of a stationary-based SDOF system which is subjected to an external force, typically called effective earthquake force (Chopra 2012). Since the effective earthquake force is equal to base shear force, earthquake energy input to SDOF system can also expressed in the form of Eq. (3)

$$E_I(t)=-\int_0^t m\cdot\ddot{u}_g(t)\cdot\dot{u}(t)dt=\int_0^t m\cdot A(t)\cdot\dot{u}(t)dt \quad (3)$$

where $A(t)$ is the pseudo acceleration. From Eq. (3), it can be observed that the equivalent static force, or the base shear, is m times $A(t)$.

In order to constitute an analogy between the input energy responses of SDOF and MDOF systems, it has been started from the modal equations of damped MDOF systems. The modal equation governing the *n*th-mode response of MDOF system to earthquake-induced ground motion can be obtained as follows by using the well-known differential equations of motion of MDOF systems:

$$\ddot{q}_n(t)+2\zeta_n\omega_n\dot{q}_n(t)+\omega_n^2 q_n(t)=-\Gamma_n\ddot{u}_g(t) \quad (4)$$

In Eq. (4), $q_n(t)$ is the *n*th modal coordinate, ω_n and ζ_n are the natural frequency and damping ratio of the *n*th mode, respectively, and Γ_n is the modal participation factor for mode n. Γ_n factor is calculated as in Eq. (5):

$$\Gamma_n=\frac{L_n}{M_n}=\frac{\phi_n{}^{\mathrm{T}}m1}{\phi_n{}^{\mathrm{T}}m\phi_n} \quad (5)$$

where M_n is the generalized mass of the *n*th natural vibration mode (i.e. modal mass), ϕ_n is the natural mode vector of the *n*th mode, m is the mass matrix and 1 is the *N*th order influence vector with each element equal to unity.

The modal equation of the *n*th-mode SDOF system, an SDOF system with vibration properties of the *n*th mode of the MDOF system, can be obtained as:

$$\ddot{D}_n(t)+2\zeta_n\omega_n\dot{D}_n(t)+\omega_n^2 D_n(t)=-\ddot{u}_g(t) \quad (6)$$

In order to derive Eq. (6), the only unknown of Eq. (4) $q_n(t)$ is related to $D_n(t)$, modal displacement of the *n*th-mode SDOF system, as in Eq. (7):

$$q_n(t)=\Gamma_n D_n(t) \quad (7)$$

The *n*th mode base shear $V_{bn}(t)$ in MDOF system is equal to the summation of equivalent static forces $f_n(t)$ associated with the *n*th-mode response and can be obtained as:

$$V_{bn}(t)=1^{\mathrm{T}}f_n(t)=M_n^*A_n(t) \quad (8)$$

where M_n^* is the base shear effective modal mass (i.e., effective modal mass) and $A_n(t)$ is the pseudo-acceleration response of the *n*th-mode SDOF system to horizontal earthquake excitation.

Taking into consideration Eq. (8), *n*th-mode input energy to MDOF system can be written as in Eq. (9):

$$E_{In}(t)=-\int_0^t M_n^*\cdot\ddot{u}_g(t)\cdot\dot{D}_n(t)dt \quad (9)$$

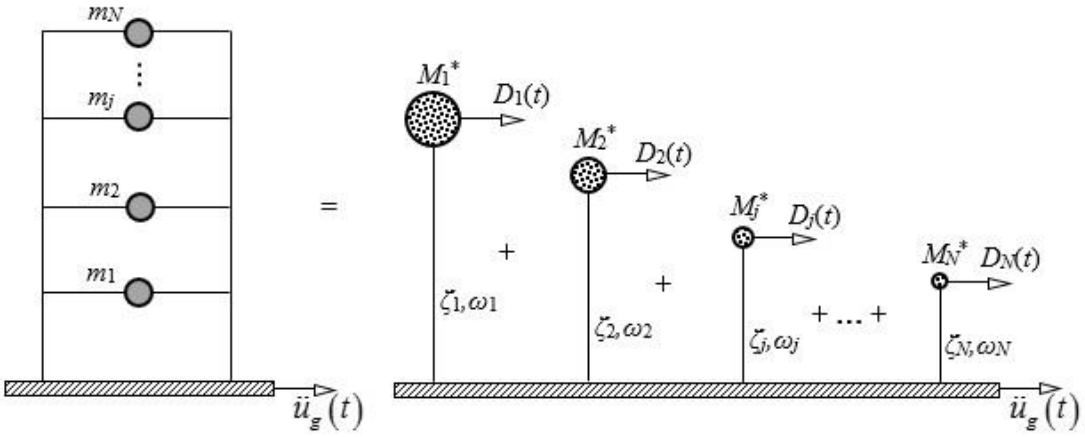

Fig. 1 *n*th-mode SDOF systems of an MDOF frame

Table 1 Major seismological parameters of records

ID	Earthquake Name	Year	Recording Station	M_w	R_{JB} (km)	V_{S30} (m/s)	*PGA* (g)	*PGV* (cm/s)	*PGV*/*PGA* (s)	I_A (m/s)
1	Imperial Valley-02	1940	El Centro Array #9	6.95	6.09	213.44	0.211	31.32	0.152	1.169
2	Parkfield	1966	Cholame - Shandon Array #5	6.19	9.58	289.56	0.368	22.12	0.062	0.628
3	Managua_ Nicaragua-01	1972	Managua_ ESSO	6.24	3.51	288.77	0.330	30.73	0.095	2.009
4	Imperial Valley-06	1979	Chihuahua	6.53	7.29	242.05	0.254	29.90	0.120	1.195
5	Westmorland	1981	Westmorland Fire Sta	5.9	6.18	193.67	0.499	35.81	0.073	1.902
6	Morgan Hill	1984	Gilroy Array #4	6.19	11.53	221.78	0.349	17.31	0.051	0.773
7	Superstition Hills-02	1987	Westmorland Fire Sta	6.54	13.03	193.67	0.211	32.33	0.156	1.198
8	Erzican_ Turkey	1992	Erzincan	6.69	0	352.05	0.496	78.16	0.161	1.789
9	Kobe_ Japan	1995	Shin-Osaka	6.9	19.14	256	0.233	21.81	0.095	0.639
10	Parkfield-02_ CA	2004	Parkfield-1-Story School Bldg	6	2.68	269.55	0.290	47.38	0.167	0.975
11	Darfield_ New Zealand	2010	Pages Road Pumping Station	7	24.55	206	0.223	56.24	0.257	1.310

The sum of $E_{In}(t)$ over all vibration modes gives the total earthquake energy input to MDOF systems, as shown in Eq. (10):

$$\left[E_I(t)\right]_{\mathbf{MDOF}} = \sum_{n=1}^{N} E_{In}(t) = \sum_{n=1}^{N}\left[-\int_0^t M_n^* \cdot \ddot{u}_g(t) \cdot \dot{D}_n(t)\,dt\right] \quad (10)$$

It is noteworthy to mention that Eq. (10) becomes identical to equations of Kalkan and Kunnath (2007) and Mezgebo (2015), if mode vectors are normalized with respect to modal mass (e.g., M_n=1). However, Eq. (10) is more general, since it is independent of how modes are normalized. The fundamental idea underlying the derivation of Eq. (10) is schematically illustrated in Fig. 1.

3. Calculation of input energy response histories

3.1 Ground motion selection and scaling

The strong ground motion data constituting the seismic input for the current study consists of a set of eleven horizontal acceleration histories selected from actual recorded events regarding earthquake magnitude, source-to-site distance, type of faulting mechanism, and soil profile type information at the recording stations. Strike-slip faulting events with a moment magnitude range of $5.9 \leq M_w \leq 7$ and source-to-site distances (R_{JB}) less than 25 km are considered. The site conditions of the selected near-fault accelerograms represent the features of site class D with regard to soil classification of NEHRP (i.e. stiff soil with 180 m/s ≤ V_{S30} ≤ 360 m/s). Pulse-like records effected by forward directivity are not included in the employed set of records.

The representative time series are selected based on a criterion where the recording spectrum provides a good match to the target spectrum over the spectral period range of interest. The quantitative measure of the overall similarity between the target spectrum and spectrum of the time series is considered as the mean squared error of the difference between the two elastic acceleration spectra. Ground motion records that satisfy the acceptance criteria specified above are compiled from NGA-West2 strong ground motion database using the web-based tool of PEER Ground Motion Database (2019). The details regarding some major seismological parameters of the selected ground motion accelerograms are summarized in Table 1, where R_{JB} is Joyner-Boore distance defined as the closest horizontal distance between the site and the surface projection of the fault rupture, V_{S30} is the average of shear wave velocity in the first 30 m of the soil at recording stations, *PGV*/*PGA* is the ratio of peak ground velocity (*PGV*) to peak ground acceleration (*PGA*), and I_A is Arias intensity of ground motion.

Table 2 Duration and intensity characteristics of scaled records

ID	Earthquake Name	T(s)	$D_{a5\text{-}95}$(s)	D_E(s)	D_E^{SR}(s)	SF	PGA^{SR}(g)	I_A^{SR}(m/s)
1	Imperial Valley-02	53.45	24.15	23.33	26.08	1.7854	0.376	3.726
2	Parkfield	43.99	7.48	3.15	5.91	1.3068	0.481	1.073
3	Managua_ Nicaragua-01	45.685	8.225	8.525	6.83	0.8763	0.289	1.543
4	Imperial Valley-06	51.58	23.98	19.73	27.59	1.4860	0.378	2.639
5	Westmorland	64.995	6.11	5.57	5.18	0.8861	0.442	1.493
6	Morgan Hill	39.99	12.545	9.36	11.32	1.3122	0.458	1.331
7	Superstition Hills-02	59.99	19.21	15.43	21.10	1.4223	0.300	2.423
8	Erzican_ Turkey	20.775	7.425	7.80	6.475	0.8314	0.413	1.237
9	Kobe_ Japan	40.95	11.59	7.54	13.70	1.7108	0.399	1.870
10	Parkfield-02_ CA	51.19	12.22	7.39	13.03	1.6464	0.477	2.634
11	Darfield_ New Zealand	53.995	21.885	20.565	26.60	1.5634	0.348	3.202

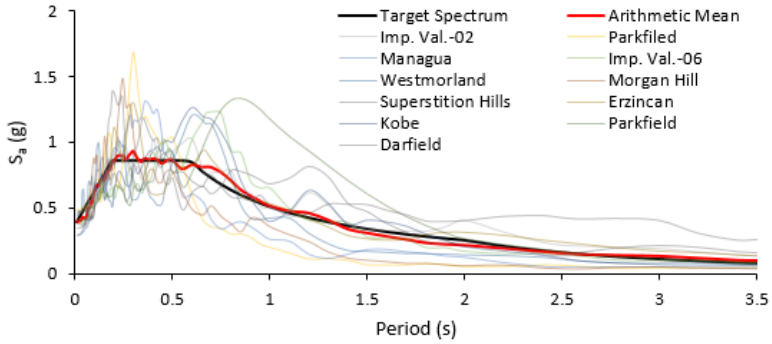

Fig. 2 Individual and average spectrum of the scaled time histories together with target spectrum

In order to minimize the mean squared error of the difference in the natural logarithm of spectral accelerations between the spectral accelerations of the record and the target acceleration spectrum, which is adopted as %5-damped Type 1 horizontal elastic ground acceleration response spectrum of EC 8 (2004) with a PGA of 0.3 g, a linear scale factor (SF) is applied to the computed response spectrum of accelerograms. Accordingly, a scale factor for each time history record is computed using Eq. (11) over periods ranging from $0.2T_1$ to $1.5T_1$ where T_1 is the fundamental period of the structure for the direction of response being analyzed:

$$\ln SF = \frac{\sum_i w(T_i) \ln\left[\frac{SA^T(T_i)}{SA^R(T_i)}\right]}{\sum_i w(T_i)} \quad (11)$$

In Eq. (11), $w(T_i)$ is the weight function that assigns relative weights to different parts of the period range of interest, $SA^T(T_i)$ and $SA^R(T_i)$ are the spectral accelerations of the record and the target spectrum, respectively. Equal weight is assigned to all periods in the specified period range used for scaling (i.e., $w(T_i)$=1) in the present study. Accordingly, the resultant scale factors are listed in Table 2, together with some duration characteristics and intensity parameters of scaled time history records. In Table 2, T is the total duration of the record, $D_{a5\text{-}95}$ denotes the significant duration evaluated as the time intervals between 5-95% of I_A, D_E and D_E^{SR} are the effective durations of unscaled and scaled earthquake strong ground motions determined based on definition of Bommer and Martínez-Perrira (1999), respectively, PGA^{SR} is peak ground acceleration of the scaled record ranging between 0.3 g and 0.481 g, I_A^{SR} is Arias intensity of scaled ground motion. The resultant scale factors range between 0.8 and 1.8, which are quite modest values. Also, the significant and the effective durations of the scaled time history record are quite close to each other.

Shown in Fig. 2 are the 5%-damped pseudo-acceleration response spectrum for each ground motion, elastic response spectrum of the arithmetic mean of the selected ensemble of ground motions and the target spectrum. A reasonably good average spectral fit to the target spectrum is achieved when the selected records are individually scaled by the factors of Table 2.

3.2 Description of MDOF systems

The numerical part of the study is composed of modal and response history analyses of SDOF systems with vibration properties (i.e. natural frequency ω_n and damping ratio ζ_n) of the nth mode of MDOF systems. 3-, 5-, and 8-story generic reinforced concrete (RC) frames with three-, and four-bays are selected for representing the MDOF systems. The length of all spans is assumed to be identical and taken as 5 m. The typical story height is 2.7 m for all floors. Rectangular beams of 250 mm width and 500 mm height, and square columns with different dimensions mainly based on story numbers are considered. Accordingly, the column dimensions are 350, 450 and 550 mm for 3-, 5-, and 8-story frames, respectively. The compressive strength of concrete is taken to be 30 MPa and

the corresponding modulus of elasticity is 32000 MPa.

The selected RC frames are 2D models of an external frame of a 3D structure and the magnitudes of gravity loads are determined accordingly. Live load participation factor is taken to be 0.30 and story weights, as well as the related seismic masses, are determined as the combination of dead loads and 30% of live loads. Accordingly, the lumped seismic floor masses are m_j=54 tons and 71 tons, and the seismic masses assigned to top floor are calculated as m_N=40.5 tons and 53.5 tons, respectively, for three-, and four-bay frames.

3.3 Modal analysis of MDOF systems

Free vibration properties of the considered MDOF systems are firstly calculated by performing modal analyses in SAP2000 (2018) software. Since the mass is lumped at floor levels and axial deformations of beam and column elements are neglected, the remained degrees of freedom (DOFs) to be considered in dynamic analysis are horizontal translation of floors. As a consequence, the first three natural periods of free vibration are listed in Table 3. Subsequently, as a part of modal analyses, modal participating mass ratios of the first three modes are also determined and given in Table 4, together with the total seismic masses. Accordingly, effective modal masses of the nth mode (M_n^*), which are essential for computing input energy response history of the considered frames in accordance with Eq. (10), can be easily calculated and utilized in seismic input energy calculations.

3.4 Input energy response histories associated with natural modes

In order to compute the total input energy, as well as the nth-mode input energy, to the considered MDOF systems by means of the derived equation, the relative velocity response $\dot{D}_n(t)$ of the nth-mode SDOF systems is computed by using PRISM (2010), a software for seismic response analysis of SDOF systems. Subsequently, energy response histories of the nth-mode SDOF systems and the total earthquake energy input to MDOF systems are computed by means of a custom MS Excel program developed by the author. Fig. 3 displays the relative input energy time-variation (i.e., input energy response history) computed through Eq. (10) for the considered frames subjected to the scaled ground motion records used in the study. Note that the vertical axis of the graphs shows the total input energy per mass of an MDOF system and the horizontal axis is the total duration of the record.

It is obvious that, input energy response history, as well as input energy demand, of MDOF systems depends not only on the structural properties of the system but also on the ground motion characteristics. Accordingly, when subjected to different ground motions, the same structures exhibit different structural responses in terms of input energy. This finding is consistent with previous works of Decanini and Mollaioli (1998), Khashaee *et al*. (2003), Cheng *et al*. (2014) and Beiraghi (2018). Fig 3 also compares the influence of bay numbers on time history of input energy to MDOF frames subjected to the same earthquake excitation. As one can see, the bay numbers has no significant effect on time history of input energy per mass of the system, since almost all dashed lines standing for E_I/m time history of three-bay frames in Fig. 3 coincides with the solid ones, which are drawn for four-bay frames. This is mainly due to almost the same natural periods of vibration.

Table 3 Natural periods of vibration (s)

N	Three-bay frames			Four-bay frames		
	n = 1	n = 2	n = 3	n = 1	n = 2	n = 3
3	0.356	0.113	0.066	0.359	0.115	0.068
5	0.473	0.147	0.079	0.475	0.148	0.080
8	0.683	0.214	0.116	0.683	0.214	0.116

Table 4 Total masses and modal participating mass ratios

N	Three-bay frames				Four-bay frames			
	m (tons)	n = 1	n = 2	n = 3	m (tons)	n = 1	n = 2	n = 3
3	148.5	0.8959	0.0871	0.0170	195.5	0.8981	0.0857	0.0163
5	256.5	0.8375	0.1024	0.0385	337.5	0.8394	0.1017	0.0378
8	418.5	0.8077	0.1006	0.0411	550.5	0.8093	0.1002	0.0407

One of the instructive advantages of computing the input energy imposed on MDOF systems during an earthquake in terms of input energy response of nth-mode SDOF system is the estimation of the contributions of the individual modes to the input energy. Accordingly, in order to emphasize this essential character of the proposed procedure, input energy response contribution of the fundamental vibration mode is plotted together with the total input energy response histories (Fig. 4). Since no significant difference is observed in input energy responses of three-, and four-bay frames, only energy time histories of four-bay frames are shown in Fig. 4. It is quite clear that, the response history of input energy considering the fundamental mode is only slightly different than the total input energy response history. Therefore, the majority of energy input to linear MDOF system is contributed by the fundamental mode. Although the contribution of higher modes to input energy response can easily be obtained by means of Eq. (10), the input energy response of the considered frames in the higher modes is insignificant.

In order to numerically demonstrate the contribution of the fundamental mode to the total input energy response, the maximum values of energy input to MDOF systems are listed together with the maximum input energies of the fundamental mode in Table 5. Given in the last line of Table 5 are the arithmetic means of the maximum input energies associated with the fundamental mode, as well as of the maximum total input energies. Accordingly, the contribution of the fundamental mode, in average, is 99.3%, 98.7% and 97.8% for 3-, 5- and 8-story frames, respectively. As number of stories increases, the contribution of the fundamental mode to maximum input energy decreases.

3.5 Results verification

To verify the accuracy of the results, the relative input

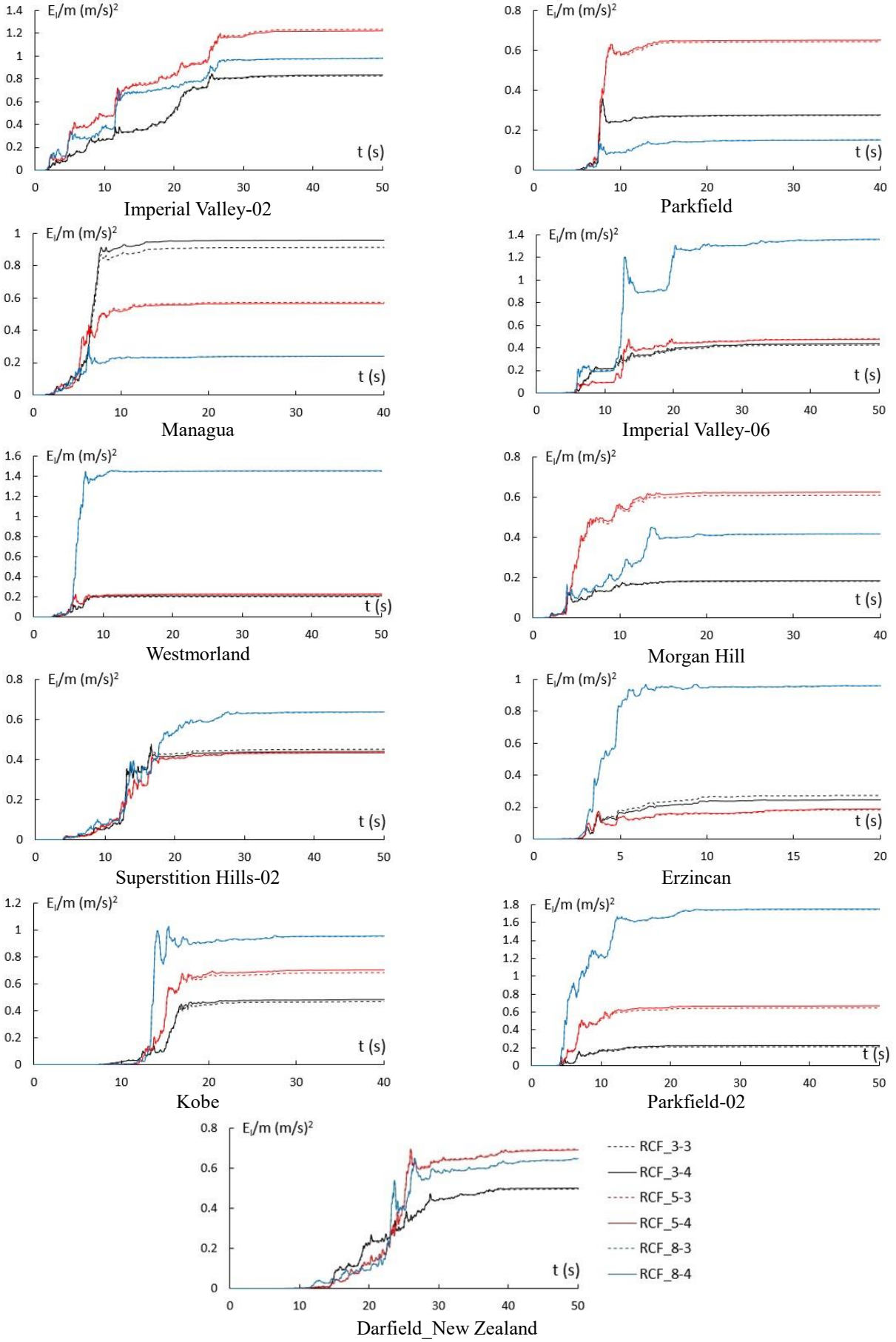

Fig. 3 Input energy response histories of different story frames

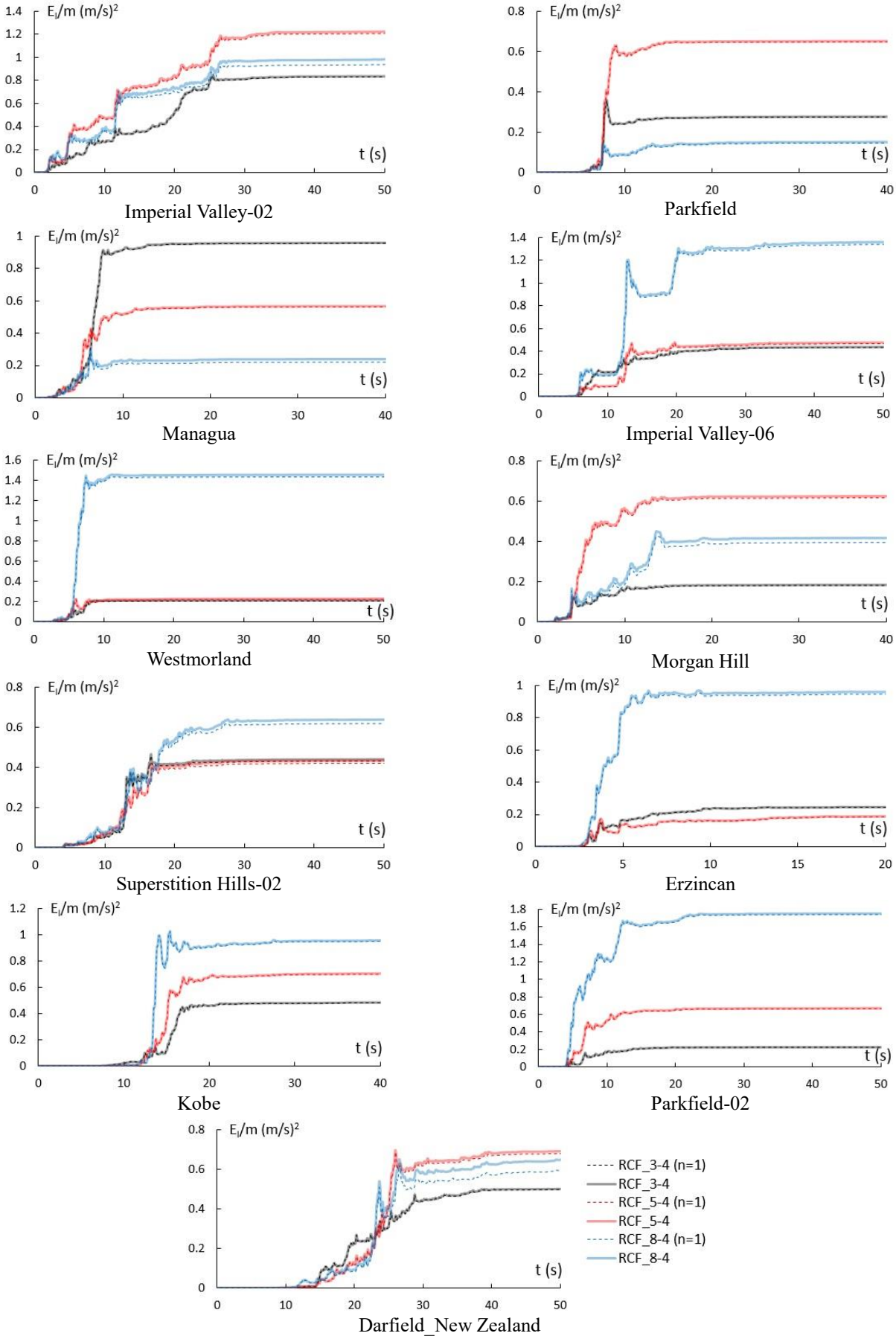

Fig. 4 Contribution of fundamental mode, $n = 1$

Table 5 Maximum input energies of the fundamental mode and maximum total input energies

EQ ID	Three-bay frames						Four-bay frames					
	$N = 3$		$N = 5$		$N = 8$		$N = 3$		$N = 5$		$N = 8$	
	$[E_I/m]_{MDOF}$	$[E_I/m]_{n=1}$	$[E_I/m]_{MDOF}$	$[E_I/m]_{n=1}$	$[E_I/m]_{MDOF}$	$[E_I/m]_{n=1}$	$[E_I/m]_{MDOF}$	$[E_I/m]_{n=1}$	$[E_I/m]_{MDOF}$	$[E_I/m]_{n=1}$	$[E_I/m]_{MDOF}$	$[E_I/m]_{n=1}$
1	0.8379	0.8340	1.2367	1.2223	0.9813	0.9366	0.8466	0.8422	1.2230	1.2080	0.9829	0.9384
2	0.3547	0.3537	0.6436	0.6402	0.1516	0.1463	0.3593	0.3583	0.6517	0.6483	0.1518	0.1466
3	0.9134	0.9106	0.5738	0.5695	0.3037	0.2883	0.9582	0.9554	0.5666	0.5623	0.3042	0.2888
4	0.4254	0.4220	0.4788	0.4703	1.3573	1.3374	0.4362	0.4326	0.4772	0.4688	1.3598	1.3400
5	0.2012	0.1968	0.2224	0.2139	1.4538	1.4336	0.2136	0.2093	0.2289	0.2215	1.4565	1.4364
6	0.1821	0.1794	0.6092	0.6011	0.4494	0.4266	0.1840	0.1814	0.6244	0.6161	0.4501	0.4275
7	0.4782	0.4708	0.4360	0.4228	0.6382	0.6192	0.4661	0.4583	0.4344	0.4216	0.6393	0.6204
8	0.2734	0.2726	0.1838	0.1815	0.9662	0.9540	0.2461	0.2451	0.1881	0.1857	0.9680	0.9558
9	0.4692	0.4669	0.6833	0.6779	1.0259	1.0218	0.4839	0.4815	0.7037	0.6986	1.0278	1.0238
10	0.2108	0.2096	0.6450	0.6405	1.7470	1.7358	0.2243	0.2229	0.6686	0.6642	1.7503	1.7391
11	0.4964	0.4930	0.6967	0.6873	0.6491	0.6042	0.5005	0.4969	0.6959	0.6866	0.6501	0.6054
Mean	0.4402	0.4372	0.5827	0.5752	0.8839	0.8640	0.4472	0.4440	0.5875	0.5801	0.8855	0.8657

Table 6 Maximum $[E_I/m]_{MDOF}$ values of Eqs. (10) and (12)

EQ ID	Three-bay frames						Four-bay frames					
	Eq. (10)			Eq. (12)			Eq. (10)			Eq. (12)		
	$N = 3$	$N = 5$	$N = 8$	$N = 3$	$N = 5$	$N = 8$	$N = 3$	$N = 5$	$N = 8$	$N = 3$	$N = 5$	$N = 8$
1	0.8379	1.2367	0.9813	0.8379	1.2350	0.9824	0.8466	1.2230	0.9829	0.8477	1.2256	0.9833
2	0.3547	0.6436	0.1516	0.3547	0.6447	0.1523	0.3593	0.6517	0.1518	0.3599	0.6512	0.1521
3	0.9134	0.5739	0.3037	0.9115	0.5730	0.3025	0.9582	0.5666	0.3042	0.9642	0.5679	0.3038
4	0.4254	0.4788	1.3573	0.4251	0.4786	1.3604	0.4362	0.4772	1.3598	0.4376	0.4778	1.3608
5	0.2012	0.2224	1.4538	0.2006	0.2234	1.4564	0.2136	0.2289	1.4565	0.2153	0.2280	1.4572
6	0.1821	0.6092	0.4494	0.1821	0.6111	0.4510	0.1840	0.6244	0.4501	0.1845	0.6229	0.4510
7	0.4782	0.4360	0.6382	0.4790	0.4360	0.6418	0.4661	0.4344	0.6393	0.4640	0.4345	0.6409
8	0.2734	0.1838	0.9662	0.2749	0.1844	0.9676	0.2461	0.1881	0.9681	0.2418	0.1876	0.9684
9	0.4692	0.6833	1.0259	0.4687	0.6859	1.0290	0.4839	0.7037	1.0278	0.4862	0.7012	1.0289
10	0.2108	0.6450	1.7470	0.2103	0.6481	1.7582	0.2243	0.6686	1.7503	0.2267	0.6658	1.7548
11	0.4964	0.6967	0.6491	0.4965	0.6965	0.6538	0.5005	0.6959	0.6501	0.5011	0.6965	0.6529
Mean	0.4402	0.5827	0.8839	0.4401	0.5833	0.8869	0.4472	0.5875	0.8855	0.4481	0.5872	0.8867

energy time histories of the considered frames are directly computed from linear time history analysis of MDOF systems. The energy input to MDOF systems is computed through Eq. (12), which can be obtained by integrating the right-hand side of the governing equation of motion of an MDOF system subjected to horizontal earthquake excitation over relative displacement of seismic masses. The time-integral form of the aforementioned equation is:

$$\left(E_I\right)_{\mathbf{MDOF}} = -\int_0^t \dot{\mathbf{u}}^{\mathbf{T}}\left(t\right)\cdot\mathbf{m}\cdot 1\cdot\ddot{u}_g\left(t\right)dt \qquad (12)$$

where **m** is the mass matrix and ***ü*****$_g$*****(t)*** is the velocity vector.

In implementation of Eq. (12), the velocity response histories of RC frames are obtained through linear time history analysis performed in SAP2000 (2018) and consequently, energy response histories of frames are computed by means of a MS Excel program developed by the author.

Table 6 compares the maximum input energy computed using Eq. (10) from elastic time history analysis of *n*th-mode SDOF systems with the input energy computed using Eq. (12) from linear time history analysis of the MDOF systems. It is clear that, the results are highly consistent, both for the individual ground motion records and the arithmetic mean. The slight differences are believed to originate mostly from the numerical methods used by SAP2000 (2018) and PRISM (2010) to compute the dynamic response.

3.6 Comparison with NLTH results

The computed elastic input energies are compared with the energy input to nonlinear MDOF systems. First, the considered moment resisting frames are designed according to horizontal elastic ground acceleration response spectrum employed in ground motion selection and scaling. The equivalent lateral forces used in seismic design are determined as a result of response spectrum analysis. Geometric properties and section details of the frames are taken as described previously and the yield strength of reinforcement steel is assumed to be 420 MPa.

Effective stiffness values of cracked RC sections are determined according to Turkish Seismic Design Code (TSDC 2018). The fundamental periods calculated by eigenvalue analysis are 0.51 s, 0.72 s and 1.08 s for 3-, 5- and 8-story frames, respectively. Beams and columns are modeled as nonlinear structural components with lumped plasticity by assigning plastic hinges at both ends. Force-displacement capacity boundaries of the components are defined in accordance with nonlinear modelling provisions of ASCE 41-13 (2014). Accordingly, two-dimensional nonlinear analytical model of each frame is created in SAP2000 (2018) platform.

Table 7 Total E_I/m values of nonlinear MDOF systems

EQ ID	Three-bay frames			Four-bay frames		
	$N=3$	$N=5$	$N=8$	$N=3$	$N=5$	$N=8$
1	1.3733	0.9869	1.2947	1.3761	0.9886	1.2963
2	0.1917	0.1787	0.1369	0.1920	0.1788	0.1369
3	0.3578	0.2738	0.2150	0.3583	0.2740	0.2150
4	0.9859	1.3124	0.9786	0.9880	1.3150	0.9799
5	0.6133	0.4052	0.2214	0.6146	0.4058	0.2224
6	0.4007	0.3569	0.2002	0.4014	0.3574	0.2004
7	0.7354	0.9842	0.9695	0.7368	0.9861	0.9710
8	0.3967	0.4035	0.4596	0.3974	0.4042	0.4603
9	0.8694	0.6777	0.8236	0.8714	0.6791	0.8248
10	1.2045	1.7776	1.3589	1.2073	1.7814	1.3611
11	0.7895	1.0928	1.2557	0.7911	1.0948	0.6917
Mean	0.7198	0.7682	0.7195	0.7213	0.7696	0.6691

Table 8 Ratios of mean inelastic to elastic input energy

Three-bay frames			Four-bay frames		
$N=3$	$N=5$	$N=8$	$N=3$	$N=5$	$N=8$
1.64	1.32	0.81	1.61	1.31	0.76

Nonlinear time history (NLTH) analyses of frames are performed by using the time histories of the scaled ground motions compatible with the target elastic design acceleration spectrum. Viscous damping ratio is taken as 5% and Rayleigh damping model, which assumes that the damping is proportional to a linear combination of the stiffness and mass (Chopra 2012), is used in NLTH analyses. As a result of 66 NLTH analyses (six frames and eleven ground motion records) performed, the nonlinear velocity response of floor masses is obtained. Consequently, energy response histories of nonlinear systems are computed by means of a MS Excel program developed by the author.

The computed elastic and inelastic input energy response histories of 3- and 8-story three bay frames from Darfield_New Zealand (2010) and Parkfield (1966) earthquakes are shown in Fig. 5. The inelastic input energy demand of Darfield_New Zealand (2010) earthquake on three-story three bay frame (F3-3) is found to be higher than the elastic one. It can be observed from Fig. 5 that the inelastic input energy demand of Parkfield (2010) earthquake on eight-story three bay frame (F8-3) is lower than the elastic. Although not observed for each individual record, the trends in Fig. 5 are mainly common for 3- and 8-story frames.

Given in Table 7 are the total input energy per mass of nonlinear MDOF systems and their arithmetic mean. Input energies of linear elastic and inelastic systems are quite different, when compared for individual records. However, the comparison of mean values reveals that the elastic input energies computed for 3- and 5-story frames are higher than inelastic ones, whereas the inelastic input energy is found to be lower than the elastic input energy in case of 8-story frames. This is consistent with the results of a recent study developed by Alıcı and Sucuoğlu (2018), where it is found that for short period systems reducing the lateral strength of the system increases input energy demand and for inelastic systems with medium and long periods near-fault input

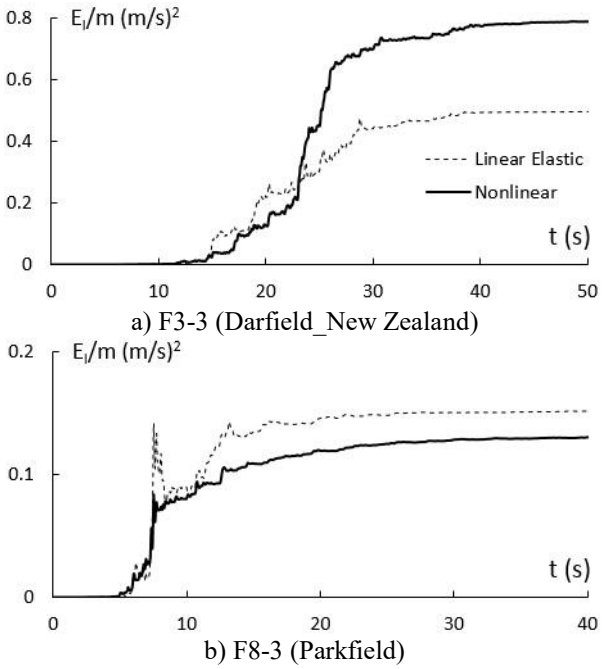

Fig. 5 The computed elastic and inelastic input energy response histories of 3- and 8-story three bay frames from Darfield_New Zealand (2010) and Parkfield (1966) earthquakes

energy reduces. Also, the inelastic input energy is found to be higher than the elastic one below a certain critical value of the period, which depends on soil class, by Decanini and Mollaioli (2001). Accordingly, it can be concluded that the input energy imposed on nonlinear MDOF structures with short to medium period (3- and 5-story frames in the study) is higher than elastic input energy. For longer period structures (8-story frames in the study), the mean inelastic input energy is lower than the elastic one.

The ratio of mean inelastic to elastic input energy values are presented in Table 8. For 3- and 5-story frames, the ratio is greater than 1. However, for 8-story frames, the ratio of inelastic to elastic input energy is less than 1, which means that the inelastic input energy demand is lower than the elastic one. Inelastic to elastic input energy ratios computed for MDOF systems are reasonably consistent with those computed by Alıcı and Sucuoğlu (2018) for SDOF systems with strength reduction factors R=4 and R=6.

4. Conclusions

An equation computing the input energy response of MDOF systems in terms of the input energy responses of nth-mode SDOF system is derived based on the analogy between the input energy responses of SDOF and MDOF systems. The main advantage of the equation is its independence from how natural modes of vibration are normalized. The proposed equation reduces to those of Kalkan and Kunnath (2007) and Mezgebo (2015), if natural mode vectors are normalized with respect to modal mass. Linear input energy response histories of 3-, 5-, and 8-story generic RC frames with three-, and four-bays are obtained.

It has been observed that the same structures exhibit different input energy responses, when subjected to different ground motion records. However, same story frames with different bays exhibit almost the same responses in terms of input energy. Additionally, input energy response contribution of the fundamental vibration mode is obtained. It has found that the majority of input energy is contributed by the fundamental mode (i.e. the fundamental mode provides sufficiently accurate input energies) and the contribution of higher modes can be eliminated for the considered frames. The accuracy of the numerical results is validated by the corresponding values computed from linear time history analysis of the MDOF systems and a very reasonable agreement is achieved.

It has been shown that, linear input energies of the *n*th-mode SDOF systems can be effectively used to compute the energy input to an MDOF system. The essential tasks are to perform the modal analysis of MDOF system and the time history analysis of *n*th-mode SDOF systems. The computation of energy input to MDOF systems in this manner is quite important since it removes the necessity to perform time history analysis for MDOF systems. Moreover, for design purposes, the energy demand of an MDOF system is estimated from the input energy spectra summarizing the peak values of energy input to SDOF system.

The natural period of vibration is an influential parameter on the relationship between the total input energy to nonlinear and linear elastic MDOF systems. For long period MDOF structures, the elastic input energy may be effectively correlated to the inelastic input energy. However, the results of this study are based on input energy response of regular MDOF structures to limited number of ground motion records.

References

Alıcı, F.S. and Sucuoğlu, H. (2016), "Prediction of input energy spectrum: attenuation models and velocity spectrum scaling", *Earthq. Eng. Struct. Dyn.*, **45**(13), 2137-2161. https://doi.org/10.1002/eqe.2749.

Alıcı, F.S. and Sucuoğlu, H. (2018), "Elastic and inelastic near-fault input energy spectra", *Earthq. Spectra*, **34**(2), 611-637. https://doi.org/10.1193/090817EQS175M.

Amiri, G.G., Darzi, G.A. and Amiri, J.V. (2008), "Design elastic input energy spectra based on Iranian earthquakes", *Can. J. Civ. Eng.*, **35**(6), 635-646. https://doi.org/10.1139/L08-013.

ASCE (2014). Seismic evaluation and retrofit of existing buildings (ASCE 41-13), American Society of Civil Engineers; Reston, Virginia, U.S.A.

Beiraghi, H. (2018), "Energy dissipation of reinforced concrete wall combined with buckling-restrained braces subjected to near- and far-fault earthquakes", *Iran. J. Sci. Technol., Trans. Civ. Eng.*, **42**(4), 345-359. https://doi.org/10.1007/s40996-018-0109-0.

Benavent-Climent, A., Pujades, L.G. and López-Almansa, F. (2002), "Design energy input spectra for moderate-seismicity regions", *Earth. Eng. Struct. Dyn.*, **31**(5), 1151-1172. https://doi.org/10.1002/eqe.153.

Benavent-Climent, A., López-Almansa, F. and Bravo-González, D.A. (2010), "Design energy input spectra for moderate-to-high seismicity regions based on Colombian earthquakes", *Soil Dyn. Earthq. Eng.*, **30**(11), 1129-1148. https://doi.org/10.1016/j.soildyn.2010.04.022.

Bommer, J.J. and Martínez-Pereira, A. (1999), "The effective duration of earthquake strong motion", *J. Earthq. Eng.*, **3**(2), 127-172. https://doi.org/10.1080/13632469909350343.

Cheng, Y., Lucchini, A. and Mollaioli, F. (2014), "Proposal of new ground motion prediction equations for elastic input energy spectra", *Earthq. Struct.*, **7**(4), 485-510. https://doi.org/10.12989/eas.2014.7.4.485.

Chopra, A.K. (2012), *Dynamics of Structures, Theory and Applications to Earthquake Engineering*, Prentice Hall, One Lake Street, Upper Saddle River, N.J. U.S.A.

Chou, C.C. and Uang, C.M. (2003), "A procedure for evaluating seismic energy demand of framed structures", *Earthq. Eng. Struct. Dyn.*, **32**(2), 229-244. https://doi.org/10.1002/eqe.221.

Chou, C.C. and Uang, C.M. (2004), "Evaluating distribution of seismic energy in multistory frames", *13th World Conference on Earthquake Engineering*, Vancouver, B.C., Canada, August.

Decanini, L.D. and Mollaioli, F. (1998), "Formulation of elastic earthquake input energy spectra", *Earthq. Eng. Struct. Dyn.*, **27**(12), 1503-1522, https://doi.org/10.1002/(SICI)1096-9845(199812)27:12<1503::AID-EQE797>3.0.CO;2-A.

Decanini, L., Mollaioli, F. and Mura, A. (2001), "Equivalent SDOF systems for the estimation of seismic response of multistory frame structures", *WIT Trans. Built Environ.*, **57**, 101-110. https://doi.org/ 10.2495/ERES010101.

Decanini, L.D. and Mollaioli, F. (2001), "An energy-based methodology for the assessment of seismic demand", *Soil Dyn. Earthq. Eng.*, **21**(2), 113-137. https://doi.org/10.1016/S0267-7261(00)00102-0.

Dindar, A.A., Yalçın, C., Yüksel, E., Özkaynak H. and Büyüköztürk, O. (2015), "Development of earthquake energy demand spectra", *Earthq. Spectra*, **31**(3), 1667-1689. https://doi.org/10.1193/011212EQS010M.

EC8 (2004), Eurocode 8: Design of structures for earthquake resistance-part 1: General rules, seismic actions and rules for buildings, European Committee for Standardization; Brussels, Belgium.

Ganjavi, B. and Rezagholilou, A.R. (2018), "An intensity measure for seismic input energy demand of multi-degree-of-freedom systems", *Civ. Eng. Infrastruct. J.*, **51**(2), 373-388. https://doi.org/10.7508/ceij.2018.02.008.

Gharehbaghi, S., Gandomi, A.H., Achakpour, S. and Omidvar, M.N. (2018), "A hybrid computational approach for seismic energy demand prediction", *Expert Syst. Appl.*, **110**, 335-351. https://doi.org/10.1016/j.eswa.2018.06.009.

Güllü, A., Yüksel, E., Yalçın, C., Anıl Dindar, A. and Özkaynak, H. (2017), "Experimental verification of the elastic input energy spectrum and a suggestion", *Proceedings of the Interdisciplinary Perspectives for Future Building Envelopes*, Istanbul, Turkey, May.

Güllü, A., Yüksel, E., Yalçın, C., Anıl Dindar, A., Özkaynak, H. and Büyüköztürk, O. (2019), "An improved input energy spectrum verified by the shake table tests", *Earthq. Eng. Struct. Dyn.*, **48**(1), 27-45. https://doi.org/10.1002/eqe.3121.

Habibi, A., Chan, R.W.K. and Albermani, F. (2013), "Energy-based design method for seismic retrofitting with passive energy dissipation systems", *Eng. Struct.*, **46**, 77-86. https://doi.org/10.1016/j.engstruct.2012.07.011.

Hori, N. and Inoue, N. (2002), "Damaging properties of ground motions and prediction of maximum response of structures based on momentary energy response", *Earthq. Eng. Struct. Dyn.*, **31**(9), 1657-1679. https://doi.org/10.1002/eqe.183.

Kalkan, E. and Kunnath, S.K. (2007), "Effective cyclic energy as a measure of seismic demand", *J. Earthq. Eng.*, **11**(5), 725-751. http://dx.doi.org/10.1080/13632460601033827.

Kalkan, E. and Kunnath, S.K. (2008), "Relevance of absolute and

relative energy content in seismic evaluation of structures", *Adv. Struct. Eng.*, **11**(1), 17-34. https://doi.org/10.1260/136943308784069469.

Kanno, H., Nishida, T. and Kobayashi, J. (2012), "Estimation method of seismic response based on momentary input energy considering hysteresis shapes of a building structure", *15th World Conference on Earthquake Engineering*, Lisboa, Portugal, September.

Karimzadeh, S., Ozsarac, V., Askan, A., and Erberik, M.A. (2019). "Use of simulated ground motions for the evaluation of energy response of simple structural systems", *Soil Dyn. Earthq. Eng.*, **123**,525-542. https://doi.org/10.1016/j.soildyn.2019.05.024.

Khashaee, P., Mohraz, B., Sadek, F., Lew, H.S. and Gross, J.L. (2003), "Distribution of earthquake input energy in structures", Report No. NISTIR 6903, National Institute of Standards and Technology, Gaithersburg.

Lei, C., Xianguo, Y. and Kangning, L. (2008), "Analysis of seismic energy response and distribution of RC frame structures", *The 14th World Conference on Earthquake Engineering*, Beijing, China, October.

López-Almansa, F., Yazgan, A.U. and Benavent-Climent, A. (2013), "Design energy input spectra for high seismicity regions based on Turkish registers", *Bull. Earthq. Eng.*, **11**(4): 885-912. https://doi.org/10.1007/s10518-012-9415-2.

Manfredi, G. (2001), "Evaluation of seismic energy demand", *Earthq. Eng. Struct. Dyn.*, **30**(4), 485-499. https://doi.org /10.1002/eqe.17.

Merter, O. (2019), "An investigation on the maximum earthquake input energy for elastic SDOF systems", *Earthq. Struct.*, **16**(4), 487-499. https://doi.org/10.12989/eas.2019.16.4.487.

Mezgebo, M.G. (2015), "Estimation of earthquake input energy, hysteretic energy and its distribution in MDOF structures", Ph.D. Dissertation, Syracuse University, New York.

Mezgebo, M. and Lui, E.M. (2016), "Hysteresis and soil site dependent input and hysteretic energy spectra for far-source ground motions", *Adv. Civ. Eng.*, **2016**, https://doi.org/10.1155/2016/1548319.

Mezgebo, M.G. and Lui, E.M. (2017), "A new methodology for energy-based seismic design of steel moment frames", *Earthq. Eng. Eng. Vib.*, **16**(1), 131-162. https://doi.org/10.1007/s11803-017-0373-1.

Mollaioli, F., Bruno, S., Decanini,L. and Saragoni, R. (2011), "Correlations between energy and displacement demands for performance-based seismic engineering", *Pure Appl. Geophys.*, **168**(1-2), 237-259. *https://doi.org/10.1007/s00024-010-0118-9*.

Morales-Beltran, M., Turan, G., Yildirim, U., and Paul, J. (2018), "Distribution of strong earthquake input energy in tall buildings equipped with damped outriggers", *Struct. Des. Tall Spec. Build.*, **27**(8), e1463. https://doi.org/10.1002/tal.1463.

Okur, A. and Erberik, M.A. (2012), "Adaptation of energy principles in seismic design of Turkish RC frame structures. Part I: Input energy spectrum", *15th World Conference on Earthquake Engineering*, Lisboa, Portugal, September.

Ordaz, M., Huerta, B. and Reinoso, E. (2003), "Exact computation of input-energy spectra from Fourier amplitude spectra", *Earthq. Eng. Struct. Dyn.*, **32**(4), 597-605. https://doi.org/10.1002/eqe.240.

Ozsarac, V., Karimzadeh, S., Erberik, M.A., Askan, A. (2017), "Energy-based response of simple structural systems by using simulated ground motions", *Procedia Eng.*, **199**, 236-241. https://doi.org/10.1016/j.proeng.2017.09.009.

PEER (2019), PEER Ground Motion Database, NGA-West2. Pacific Earthquake Engineering Research Center. http://ngawest2.berkeley.edu/

PRISM for Earthquake Engineering. (2010), A Software for Seismic Response Analysis of Single-Degree-of-Freedom-Systems, Version 2.0.1, Department of Architectural Engineering, INHA University.

Quinde, P., Reinoso, E. and Terán-Gilmore, A. (2016), "Inelastic seismic energy spectra for soft soils: Application to Mexico City", *Soil Dyn. Earthq. Eng.*, **89**, 198-207. https://doi.org/10.1016/j.soildyn.2016.08.004.

SAP2000 Ultimate. (2018), Integrated Solution for Structural Analysis and Design, Version 20.2.0, Computers and Structures Inc. (CSI), Berkeley, California, U.S.A.

Sari, A. (2003), "Energy considerations in ground motion attenuation and probabilistic seismic hazard studies", Ph.D. Dissertation, The University of Texas at Austin, Austin. U.S.A.

Shargh, F.H. and Hosseini, M. (2011), "An optimal distribution of stiffness over the height of shear buildings to minimize the seismic input energy", *J. Seismol. Earthq. Eng.,* **13**(1), 25-32.

Shargh, F.H., Hosseini, M. and Daneshvar, H. (2012), "An optimal distribution of stiffness over the height of buildings and its influence on the degree and distribution of earthquake induced damages and distribution of earthquake induced damages", *15th World Conference on Earthquake Engineering*, Lisboa, Portugal, September.

Shiwua, A.J., Rutman, Y. (2016), "Assessment of seismic input energy by means of new definition and the application to earthquake resistant design", *Archit. Eng.*, 1(4), 26-35. https://doi.org/10.23968/2500-0055-2016-1-4-26-35.

Surahman, A. (2007), "Earthquake-resistant structural design through energy demand and capacity", *Earthq. Eng. Struct. Dyn.*, **36**(14), 2099-2117. https://doi.org/10.1002/eqe.718.

Taflampas, I.M., Maniatakis, Ch.A. and Spyrakos, C.C. (2008), "Estimation of input seismic energy by means of a new definition of strong motion duration duration", *The 14th World Conference on Earthquake Engineering*, Beijing, China, October.

Takewaki, I. (2004), "Frequency domain modal analysis of earthquake input energy to highly damped passive control structures", *Earthq. Eng. Struct. Dyn.*, 33(**5**), 575-590. https://doi.org/10.1002/eqe.361.

Takewaki, I. and Fujita, K. (2009), "Earthquake input energy to tall and base-isolated buildings in time and frequency dual domains", *Struct. Des. Tall Spec. Build.*, **18**(6), 589-606. https://doi.org/10.1002/tal.497.

Takewaki, I. and Tsujimoto, H. (2011), "Scaling of design earthquake ground motions for tall buildings based on drift and input energy demands", *Earthq. Struct.*, **2**(2), 171-187. https://doi.org/10.12989/eas.2011.2.2.171.

Tselentis, G-A., Danciu, L. and Sokos, E. (2010), "Probabilistic seismic hazard assessment in Greece – Part 2: Acceleration response spectra and elastic input energy spectra", *Nat. Hazards Earth Syst. Sci.*, **10**(1), 41-49. https://doi.org/10.5194/nhess-10-41-2010.

TSDC (2018). Turkish seismic design code, Ministry of Public Works and Settlement; Ankara, Turkey.

Wong, K.K.F. and Yang, R. (2002), "Earthquake response and energy evaluation of inelastic structures", *J. Eng. Mech.*, **128**(3), 308-317. https://doi.org/10.1061/(ASCE)0733-9399(2002)128:3(308).

Yang, T.Y., Tung, D.P., and Li, Y. (2018), "Equivalent energy design procedure for earthquake resilient fused structures", *Earthq. Spectra*, **34**(2), 795-815. https://doi.org/10.1193/122716EQS254M.

Ye, L., Cheng, G. and Qu, Z. (2009), "Study on energy-based seismic design method and the application for steel braced frame structures", *Sixth International Conference on Urban Earthquake Engineering*, Tokyo Institute of Technology, Tokyo, Japan, March.

Zhou, Y., Song, G., Huang, S. and Wu, H. (2019), "Input energy spectra for self-centering SDOF systems", *Soil Dyn. Earthq. Eng.*, **121**, 293-305. https://doi.org/10.1016/j.soildyn.2019.03.017.

CC